Acta Cryst. (1992). A**48**, 555-562

Inversion of Convergent-Beam Electron Diffraction Patterns

BY D. M. BIRD AND M. SAUNDERS

School of Physics, University of Bath, Bath BA2 7AY, England

(*Received* 17 *October* 1991; *accepted* 7 *February* 1992)

Abstract

The problem of recovering the structure factors that contribute to a zone-axis convergent-beam diffraction pattern is discussed.. It is shown that an automated matching procedure that minimizes the sum-of-squares difference between experimental and simulated patterns is effective whether one is refining accurate structure factors in a known crystal or attempting *ab initio* structure determination. The details of the minimization method are analysed and it is shown that a quasi-Newton method that uses analytically derived gradients is particularly effective when several structure factors are varied. The inversion method for *ab initio* structure determination is tested on the [110] axis of GaP, using simulated patterns as ideal 'experimental' data.

1. Introduction

There has been a growing realization over the past few years that the matching of experimental and computed patterns has the potential to expand greatly the scope of quantitative convergent-beam electron diffraction (CBED). The basic point is that intensity measurement is essential if we want to determine the Fourier components of the crystal potential, *i.e.* the crystal *structure factors*, and the measurement of structure factors is a vital step in the development of electron crystallography as a rival to the established X-ray and neutron diffraction techniques. Two factors have made this intensity matching possible: firstly, the introduction of instrumentation for the acquisition of quantitative (and preferably energy-filtered) diffraction intensities (Zuo, Spence & Hoier, 1989; Mayer, Spence, Ernst & Möbus, 1991); secondly, the availability of the considerable computing power required to undertake a full dynamical analysis of the experimental data. The applications of intensity measurement considered to date include the following.

(i) The refinement of very accurate low-order structure factors in known crystal structures (Zuo, Spence & O'Keeffe, 1988; Zuo & Spence, 1991). Using these, it is possible to determine the valence charge distribution in the crystal and address questions such as the nature of the bonding, bond charge, ionicity *etc.* (see also Zuo, Spence & Petuskey, 1990).

(ii) The measurement of crystallographic phase invariants (*i.e.* combinations of structure-factor phases; Bird, James & Preston, 1987; Zuo, Spence & Hoier, 1989; Marthinsen, Hoier & Bakken, 1990) by detailed fitting of the intensity distribution around three- or four-beam diffraction situations.

(iii) The measurement of medium- and high-order structure factors from higher-order Laue-zone rings (Vincent, Bird & Steeds, 1984; Tanaka & Tsuda, 1990, 1991) or large-angle convergent-beam patterns (Taftø & Metzger, 1985; Vincent & Bird, 1986; Gjonnes, Boe & Gjonnes, 1990; Tomokiyo & Kuroiwa, 1990) to refine positional or occupational parameters, or to attempt a determination of unknown crystal structures (*e.g.* Vincent & Exelby, 1990).

More recently, there has been considerable interest in the possibility of the automatic matching of experimental and theoretical CBED patterns, by the minimization of some measure of the difference between the patterns. Marthinsen *et al.* (1990) attempted to minimize an R factor by a steepest-descents method, while Zuo & Spence (1991), Bird & Saunders (1991) and Tanaka & Tsuda (1991) all attempt to minimize the sum-of-squares difference using the simplex, quasi-Newton and Marquadt methods respectively. In this paper we give more details of the work described in Bird & Saunders (1991) and explain why we believe that zone-axis patterns offer more scope for structure-factor measurement than the systematic rows favoured by Zuo, Spence and co-workers. We also discuss why the quasi-Newton method with analytic gradients (Gill, Murray & Wright, 1981; Fletcher, 1987) offers the best prospect of efficient structure-factor determination, particularly when many structure factors are varied simultaneously. The problem we tackle is the *inversion* of a CBED pattern to recover the scattering potential. While the forward-direction problem, that of computing a pattern from a known structure, is now relatively straightforward, the inversion of dynamical (*i.e.* multiple) scattering intensities remains extremely difficult. As we shall show, it becomes soluble basically because there is a discrete set of potential Fourier components in a crystal and only a relatively small subset of these makes a large contribution to a typical CBED pattern. There are two related aspects to the inversion problem:

0108-7673/92/040555-08$06.00

(i) the refinement of accurate structure factors for a known crystal structure;

(ii) the recovery of sufficient structure factors in an unknown material to determine the crystal structure (*i.e. ab initio* structure determination).

Although these problems may appear at first sight to be unrelated, the same automatic pattern-matching techniques can be applied to both. The only real difference is the starting point; in (i) we have a very good idea of what the structure factors are [both elastic (Doyle & Turner, 1968) and absorptive (Bird & King, 1990) parts], while in (ii) we can assume no *a priori* knowledge. The work to date has addressed the first problem (Zuo & Spence, 1991; Tanaka & Tsuda 1991); here we address the second. In many ways this is more difficult, but in a sense it is also more fundamental - can we, with no prior information, solve a crystal structure purely by inversion of a CBED pattern? The work presented here is essentially a feasibility study to see if this problem might in principle be soluble. To that end we make no attempt to analyse real experimental data, we work with unrealistically small patterns and we ignore complicating factors such as absorption and high-order Laue-zone (HOLZ) effects.

A significant feature of the present work is that we analyse the zero-layer diffraction of a zone-axis CBED pattern. In their work on accurate structure-factor refinement, Zuo & Spence (1991) used systematic rows, while Tanaka & Tsuda (1991) analyse HOLZ diffraction in a zone-axis pattern to obtain accurate positional parameters in a known structure. Although it is not yet clear how the techniques compare, we feel that zone-axis diffraction has three advantages over systematic rows for both *ab initio* structure determination and accurate structure-factor refinement. Firstly, more structure factors contribute to a zone-axis pattern, so a larger set can be obtained from a single pattern. For example, the [100] and [110] axes in a face-centred cubic crystal include *all* structure factors out to (531). In principle, therefore, from just two experimental patterns we can determine a set of structure factors that is certainly large enough to include all the low-order factors required for analysis of bonding, and which goes a long way towards an *ab initio* structure determination. Secondly, there is considerably more information in a zone-axis pattern than in systematic diffraction. The CBED discs in a systematic row consist of fringes and the intensity information is essentially restricted to the peak intensities of this one-dimensional fringe pattern. This is to be contrasted with the fully two-dimensional character of the intensity distribution in the discs of a zone-axis pattern. The information content is a vital ingredient in the inversion procedure - it is important to have a highly over-determined problem (*i.e.* many more items of data than the number of parameters we hope to extract) if the sum-of-squares minimization is to work efficiently and to give accurate structure factors. The reduced information content of systematic rows is likely to become increasingly significant as unit cells become larger, because the CBED discs become smaller and the number of fringes is reduced. The only way to counteract this would be to increase the crystal thickness, but this would lead to an undesirable increase in the background. Thirdly, zone-axis diffraction is more dynamical than systematic diffraction in the sense that more multiple-scattering paths are open in a zone-axis situation, and zone-axis extinction lengths tend to be shorter than in one-dimensional diffraction. This has the advantage that there should be a greater sensitivity to the amplitudes and phases of the structure factors, again leading to a more accurate inversion.

The outline of the paper is as follows. In § 2 we define the sum-of-squares function that we aim to minimize and show how to calculate its gradients with respect to the structure factors that are allowed to vary. In § 3 the feasibility of carrying out *ab initio* structure determination is discussed, with reference to the [110] axis of GaP. § 4 is the discussion.

2. Sum-of-squares minimization

Zuo & Spence (1991) define the sum-of-squares difference between theoretical, $I_{\rm th}$, and experimental, $I_{\rm ex}$, intensities as

$$\chi^2 = \sum_{\mathbf{G}} \sum_i [f(\mathbf{G}, \mathbf{K}_i)/\sigma^2(\mathbf{G}, \mathbf{K}_i)] \times [I_{\rm ex}(\mathbf{G}, \mathbf{K}_i) - cI_{\rm th}(\mathbf{G}, \mathbf{K}_i)]^2, \quad (1a)$$

where the $\mathbf{G}$ sum is over the diffracted discs in the zone-axis CBED pattern and the i sum is over the orientations (described by transverse wavevector $\mathbf{K}_i$) within each disc. Each experimental intensity measurement has an associated weighting factor, $f(\mathbf{G}, \mathbf{K}_i)$, and variance, $\sigma^2(\mathbf{G}, \mathbf{K}_i)$, which is usually taken to be $I_{\rm ex}(\mathbf{G}, \mathbf{K}_i)$. We experience no problems with σ^2 going to zero in our current calculations, since computed intensities do not go to zero. When using true experimental data, obtained for example using a 12 bit CCD camera (Mayer *et al.*, 1991), the intensity would be an integer in the range 0 to 4096 and it would be necessary to ensure that any zero intensities were set to 1 to prevent (1*a*) blowing up. Finally, c is a normalization coefficient. In addition to (1*a*), we have also used the function

$$\chi^2 = \sum_{\mathbf{G}} \sum_i f(\mathbf{G}, \mathbf{K}_i)\{[I_{\rm ex}(\mathbf{G}, \mathbf{K}_i)]^{1/2} - c[I_{\rm th}(\mathbf{G}, \mathbf{K}_i)]^{1/2}\}. \quad (1b)$$

The relationship between (1*a*) and (1*b*) can be seen if (1*a*) is written in the form (with $\sigma^2 = I_{\rm ex}$)

$$\chi^2 = \sum_{\mathbf{G}} \sum_i f(\mathbf{G}, \mathbf{K}_i)\{[I_{\rm ex}(\mathbf{G}, \mathbf{K}_i)]^{1/2} - c[I_{\rm th}(\mathbf{G}, \mathbf{K}_i)]^{1/2} \times [I_{\rm th}(\mathbf{G}, \mathbf{K}_i)/I_{\rm ex}(\mathbf{G}, \mathbf{K}_i)]^{1/2}\}^2. \quad (1c)$$

It is clear that, provided the experimental and theoretical intensities are closely matched, the difference between (1*a*) and (1*b*) is small. For reasons that will be explained later, we have found it more convenient to work with (1*b*) when considering *ab initio* structure determination. The theoretical intensities $I_{\rm th}$ are calculated from amplitudes $A_{\mathbf{G}}(\mathbf{K}_i)$, which are expressed in terms of the Bloch-wave coefficients $C_{\mathbf{G}}^{(j)}(\mathbf{K}_i)$ of the many-beam equations, *i.e.*

$$I_{\rm th}(\mathbf{G},\mathbf{K}_i)=|A_{\mathbf{G}}(\mathbf{K}_i)|^2 \qquad (2a)$$

$$A_{\mathbf{G}}(\mathbf{K}_i)=\sum_j C_{\mathbf{0}}^{(j)*}(\mathbf{K}_i)C_{\mathbf{G}}^{(j)}(\mathbf{K}_i) \times \exp\left[-is^{(j)}(\mathbf{K}_i)t/2k\right], \qquad (2b)$$

where

$$\sum_{\mathbf{H}}\{[(\mathbf{K}_i+\mathbf{G})^2-s^{(j)}(\mathbf{K}_i)]\delta_{\mathbf{G},\mathbf{H}}+U_{\mathbf{G}-\mathbf{H}}\}C_{\mathbf{H}}^{(j)}(\mathbf{K}_i)=0. \qquad (3)$$

In (2*b*), t is the crystal thickness and k the fast-electron wavevector, and in (3) the structure factors $U_{\mathbf{G}}$ are defined by

$$U(\mathbf{R})=(2\gamma m_0/\hbar^2)V(\mathbf{R})=\sum_{\mathbf{G}} U_{\mathbf{G}}\exp(i\mathbf{G}\cdot\mathbf{R}), \qquad (4)$$

where $V(\mathbf{R})$ is the projected crystal potential at the given zone axis. As discussed above, we ignore HOLZ effects, so all the vectors which appear in (2)–(4) are strictly two-dimensional. The notation used is the same as in Bird (1989), where further details of the background theory may be found. We also neglect absorption, which ensures that $V(\mathbf{R})$ in (4) is real.

It is clear from (2) and (3) that the only inputs to the theoretical intensities are the set of structure factors $\{U_{\mathbf{G}}\}$, the crystal thickness, the accelerating voltage and the crystal lattice parameters [which are needed for calculation of $(\mathbf{K}+\mathbf{G})^2$]. The accelerating voltage and lattice parameters can be measured independently by standard CBED techniques and so, in general, only the structure factors and thickness need be treated as unknown parameters. In the present work, where we use simulated patterns as ideal 'experimental' data, the thickness is fixed at the known value. With real data, this cannot be done, but the inclusion of thickness as a fitting variable is straightforward, as discussed below. Also, in (1) we put $f=1$ for all $\mathbf{G}$ and $\mathbf{K}$ and, because the intensity scale of the 'experimental' data is known, we set $c=1$. Again, the extension to real data is straightforward.

Many methods exist for the minimization of sum-of-squares functions like χ^2 (*e.g.* Fletcher, 1987). The basic idea is to use χ^2 as a measure of the difference between experimental and simulated patterns and to minimize χ^2 by varying the inputs to the $I_{\rm th}$ calculation. As discussed above, these consist of a set of structure factors together with the crystal thickness. The set of parameters that minimize χ^2 then represents the best estimate of these variables. Zuo & Spence (1991) show how the error in these values can also be estimated. The best minimization method depends on the problem to be solved, but Fletcher (1987) recommends using the quasi-Newton method, and this method is implemented in the NAG library (Gill, Murray & Wright, 1981). Zuo & Spence (1991) recommend using the simplex method because they experienced unreliability with their quasi-Newton program, but we have found no such difficulties with the NAG routine. Although robust, the simplex method is relatively slow and the minimization time scales exponentially with the number of parameters that are varied. In contrast, the quasi-Newton method has an approximately linear scaling. The scaling is a significant factor because it is important to vary as many structure factors as possible to obtain the best fit; with the 20 or more parameters we may want to vary in a zone-axis calculation (see below), the simplex method becomes impractically slow.

The quasi-Newton method requires the *gradients* of $I_{\rm th}$ with respect to the parameters that are varied. These can be found using finite differences, but analytic gradients are far superior if they are available and they do not take an excessive amount of time to compute. In our case, we need to calculate

$$\partial A_{\mathbf{G}}(\mathbf{K}_i)/\partial U_{\mathbf{H}} \quad \text{and} \quad \partial A_{\mathbf{G}}(\mathbf{K}_i)/\partial t \qquad (5)$$

for all $A_{\mathbf{G}}(\mathbf{K}_i)$ that are included in the pattern and for all $U_{\mathbf{H}}$ that are treated as fitting parameters. Having obtained these gradients of the diffracted amplitudes, those of the intensities follow immediately. The gradient with respect to t is found trivially by differentiation of (2*b*), so the problem reduces to finding $\partial A_{\mathbf{G}}/\partial U_{\mathbf{H}}$. To do this, we use first-order perturbation theory, as described by Bird (1990) in the context of absorptive potentials (see also Zuo, 1991). The change in amplitude $\delta A_{\mathbf{G}}$ caused by any small additional potential $\delta U(\mathbf{R})$ which has the same periodicity as the basic potential in (4) is given by

$$\delta A_{\mathbf{G}}=\sum_{j,j'}(i\delta U_{jj'}t/2k)C_{\mathbf{0}}^{(j)*}C_{\mathbf{G}}^{(j')} \times\exp\{-i[s^{(j)}+s^{(j')}]t/4k\} \times\sin\{[s^{(j)}-s^{(j')}]t/4k\}/\{[s^{(j)}-s^{(j')}]t/4k\} \qquad (6)$$

with

$$\delta U_{jj'}=\sum_{\mathbf{G},\mathbf{G}'}(1/A_c)\int_{\rm cell}{\rm d}\mathbf{R}\,C_{\mathbf{G}'}^{(j')*} \times\exp(-i\mathbf{G}'\cdot\mathbf{R})\delta U(\mathbf{R})C_{\mathbf{G}}^{(j)}\exp(i\mathbf{G}\cdot\mathbf{R}). \qquad (7)$$

In (7), the integral is over a projected unit cell, whose area is A_c (Bird, 1989). In the present case, we are interested in the change in amplitude when a structure factor $U_{\mathbf{H}}$ is changed to $U_{\mathbf{H}}+\delta U_{\mathbf{H}}$. $\delta U(\mathbf{R})$ then becomes $\delta U_{\mathbf{H}}\exp(i\mathbf{H}\cdot\mathbf{R})$, giving

$$\delta U_{jj'}(\mathbf{H})=\delta U_{\mathbf{H}}\sum_{\mathbf{G}}C_{\mathbf{G}+\mathbf{H}}^{(j')*}C_{\mathbf{G}}^{(j)}. \qquad (8)$$

Although this analytic evaluation of the integral in (7) may appear to be useful, it is in fact better to work directly with (7) rather than use (8). The reason lies in the number of operations, and therefore the computing time, required to evaluate $\delta U_{jj'}(\mathbf{H})$ for all j, j' and $\mathbf{H}$. If we have an N-beam calculation and we are varying M structure factors [*i.e.* there are M $\mathbf{H}$s in (8)], the computing time of (8) scales as N^3M. With finite differences, the same gradients can be calculated in a similar time because each diagonalization scales as N^3 and M of these are required as each structure factor is varied. Tests show that the overheads associated with the computation of analytic gradients using (6) and (8) means that they take a little longer than the equivalent finite-difference method. Although this might be acceptable, given the greater accuracy and reliability of analytic gradients, it would clearly be advantageous to improve the efficiency of the gradient calculation. This can be achieved by using fast Fourier transforms to evaluate (7). The sums over $\mathbf{G}$ and $\mathbf{G}'$ represent Fourier transforms of the Bloch-wave coefficients, to give the Bloch waves in real space. These transforms can be computed and stored for each Bloch state j; this takes of order $N^2 \log N$ operations (*i.e.* $N \log N$ for each of N states). The $\mathbf{R}$ integral in (7) is then just a further Fourier transform of the product of two real-space Bloch states, which gives $\delta U_{jj'}(\mathbf{H})$ for all $\mathbf{H}$. For each of the N^2 j and j' combinations, this transform requires of order $N \log N$ operations, making this part of the computation scale as $N^3 \log N$. The gradient calculation dominates in terms of computer time, leading to the whole calculation scaling roughly as $N^3 \log N$. Despite the redundancy of calculating $\delta U_{jj'}$ for all $\mathbf{H}$ rather than the M that are required, tests show that the Fourier transform method is significantly faster than using finite differences when a large number of gradients is required.

Once the gradients have been calculated, the minimization procedure is straightforward. Given starting values for the set of structure factors that we choose to vary, the NAG routine *E04GBF* is used to minimize χ^2. It is important to note that the same procedure can be used whether we are attempting *ab initio* structure determination or accurate structure-factor refinement. The only difference is in the initial values of U_G that are used in the many-beam equations (3). When refining a known crystal, it is reasonable to use structure factors derived, in the usual way, from tabulated atomic scattering factors (Doyle & Turner, 1968). If absorption is included, the equivalent form factors are given by Bird & King (1990). Those structure factors that are not varied are then fixed at these initial values, while a chosen set are allowed to vary to minimize χ^2. However, in the case of *ab initio* structure determination we can assume no prior knowledge of the structure factors and those that are not included in the minimization of χ^2 are set to zero. A problem arises in that we also do not know how to choose starting values for the structure factors that do vary. This is heightened by the fact that (as will be discussed in the next section) χ^2 has several local minima in the multi-dimensional structure-factor space; with any set of starting values it is impossible to know whether one will find the global minimum or one of the local minima. This is a well known problem in optimization theory (*e.g.* Fletcher, 1987) and there is no general solution. In the work discussed in the next section we generate a number of random starting points and assume that the overall minimum from all these runs is the true global minimum. Our present method is extremely crude and a number of alternative schemes are available, *e.g.* simulated annealing, restarting from local minima *etc.* (Fletcher, 1987). Nevertheless, we have found our method to be satisfactory for these preliminary calculations.

3. Application to GaP [110]

To investigate the feasibility of *ab initio* inversion of a CBED pattern we use as our example the [110] axis of GaP. Figs. 1(*a*) and (*b*) show CBED patterns calculated using structure factors derived from Doyle & Turner (1968) scattering factors. In both patterns the thickness is 250 Å and the accelerating voltage is 300 kV. Fig. 1(*a*) is calculated with 43 beams in the many-beam equations and Fig. 1(*b*) is the result of a 19-beam calculation. The indexing of Fig. 1(*b*) is shown in Fig. 1(*c*). Neither pattern includes absorption or HOLZ effects. The 43-beam pattern is essentially converged with respect to the number of beams in the calculation. It can be seen that there are some differences between the 43- and 19-beam calculations, but the basic structure is similar. We have chosen to work with the smaller pattern to reduce the computing time required in the minimization procedure.

GaP [110] has been chosen for this study because, even though the crystal structure is simple, it represents a rather difficult test case. GaP is non-centrosymmetric and the [110] axis has a non-centric projection. The projected potential is shown in Fig. 1(*d*) and displays the familiar dumb-bell structure, with the heavier Ga strings forming a stronger potential than lighter P-atom strings. Because GaP is non-centrosymmetric, the structure factors that make up the projected potential and enter the many-beam equations have non-trivial *phases* as well as amplitudes. To reconstruct the potential, it will be necessary to obtain these phases; in effect, solving the infamous 'phase problem' of X-ray crystallography. The task we are faced with is clear from Figs. 1(*b*) and (*d*). The forward-direction calculation, from Fig. 1(*d*) to Fig. 1(*b*), is straightforward if the structure factors are known. However, the inverse problem is much

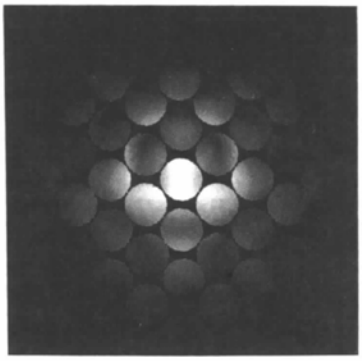

(*a*)

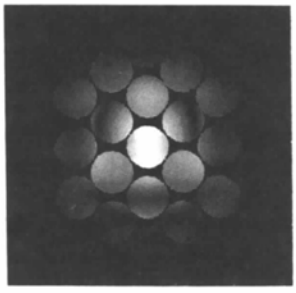

(*b*)

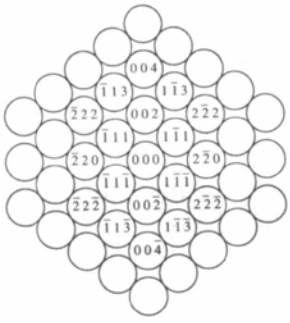

(*c*)

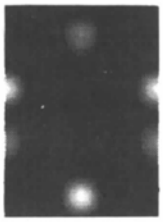

(*d*)

Fig. 1. GaP [110] CBED pattern calculated using (*a*) 43 beams and (*b*) 19 beams in the many-beam equations. Thickness is 250 Å and accelerating voltage is 300 kV. (*c*) Indexing of (*b*). (*d*) Projected potential for GaP [110].

more difficult; can we, with no other information, go *backwards* from the CBED pattern to the projected potential? In other words, can we extract from Fig. 1(*b*) a sufficient number of structure factors (both amplitudes and phases) with sufficient accuracy to reconstruct the potential of Fig. 1(*d*)?

The full list of structure factors that enter the many-beam equations in a 19-beam calculation is $(1\bar{1}1)$, (002), $(2\bar{2}0)$, $(1\bar{1}3)$, $(2\bar{2}2)$, (004), $(3\bar{3}1)$, $(2\bar{2}4)$, $(3\bar{3}3)$, $(1\bar{1}5)$, $(4\bar{4}0)$, (006), $(4\bar{4}2)$, $(3\bar{3}5)$, $(2\bar{2}6)$, $(4\bar{4}4)$, $(1\bar{1}7)$ and (008), together with their $-\mathbf{G}$ and mirror-related equivalents. In principle, each has an amplitude and phase, but in practice we can fix the origin to make some of them real. The [110] axis has a mirror plane lying through the (002) discs and we put the origin on the associated mirror in real space (*i.e.* through the axis of the dumb-bells in Fig. 1*d*). This choice forces $U_{(2\bar{2}0)}$ and $U_{(4\bar{4}0)}$ to be real, although their amplitudes can still be of either sign. There remains one free parameter that determines the origin in the [001] direction; we fix this by forcing the $(1\bar{1}1)$ structure factor also to be real. This choice of origin is consistent with the projected potential shown in Fig. 1(*d*). The 19-beam pattern is therefore constructed from 33 structure-factor parameters; 15 structure factors have amplitude and phase, while 3 have amplitude only. When working with real experimental data, the crystal thickness will of course be another free parameter, but here we keep it fixed at its known value of 250 Å. The reason for using this small thickness arises from the problem with local minima in χ^2. Tests show that the number of local minima rises with thickness, so that finding the global minimum (with some degree of certainty) at 500 Å takes roughly twice as many minimization runs as at 250 Å. A lower limit to the thickness is forced by the requirement that there should be sufficient *information* in the CBED pattern to extract the required structure factors. Very thin crystals give featureless CBED discs, and if there were only one intensity measurement available from each disc it is clearly impossible to determine 33 structure-factor parameters. The thickness must therefore be sufficiently large to produce structure (*i.e.* intensity variation) in the CBED discs, as observed in Fig. 1(*b*). For GaP [110] we have found 250 Å to be an ideal compromise between having sufficient information for the inversion and avoiding too many problems with local minima. In our calculations the CBED discs are sampled with 13 orientations that are taken uniformly over the area of each disc. Only intensities that are not mirror-related are included in the calculation of χ^2, leading to a total of 136 independent bits of intensity information. It can be seen that the problem is highly over-determined, with 136 items of data being available to fit a maximum of 33 parameters. In practice (see below) we attempt to fit at most 18 parameters, which improves the statistics still further.

As discussed above, the minimization of χ^2 proceeds by choosing a set of structure factors to vary and giving these random starting values within a reasonable range (0 to 3 $Å^{-2}$ for amplitudes and 0 to 2π for phases). All other U_Gs in the many-beam equations are set to zero. Calculations have been carried out allowing 4, 5, 6, 7, 8 and 10 structure factors to vary; these involve variation with respect to 6, 8, 10, 12, 14 and 18 parameters respectively. 150 minimization runs are performed in each case to build up a picture of the minima that occur in the multi-dimensional space of χ^2. The global minimum then becomes apparent; it usually has a considerably lower χ^2 than the local minima and it is found in a larger proportion of the runs. The largest calculation therefore involves performing 150 minimizations in an 18-dimensional space. This takes of order 30 h CPU on a 2Mflop SUN workstation.

The results are presented in Table 1, which shows the values of the structure-factor amplitudes (a) and phases (φ) that minimize χ^2. Also shown are the ideal results (*i.e.* those used to generate Fig. 1*b*) and the final values of χ^2 (SSQ). In producing these results we use the form of χ^2 given in (1*b*) rather than the form (1*a*) used by Zuo & Spence (1991). The reason lies in the number of times the global minimum is found in each calculation. Using (1*b*) and varying four structure factors, the global minimum is found in seven of the 150 runs. With 5, 6, 7, 8 and 10 structure factors this becomes 9, 5, 3, 3 and 1 respectively. The overall decrease reflects the increase in the number of local minima as the number of fitting parameters is increased. This is due to the decreasing sensitivity of the CBED pattern to the higher-order structure factors. For example, the structure factors are added in the last three calculations [namely $(3\bar{3}1)$, $(2\bar{2}4)$, $(1\bar{1}5)$ and $(3\bar{3}3)$] do not have associated discs in the pattern and we cannot expect the same degree of sensitivity to these as we find with the lower-order U_G. It is therefore not surprising that the number of local minima increases with the number of fitting parameters and that it hence becomes more difficult to find the best fit. Interestingly, we find that when using the χ^2 of (1*a*) this problem with local minima is considerably magnified. When 4, 5, 6 and 7 structure factors are varied, the global minimum is found in only 5, 1, 1 and 0, respectively, of the 150 runs. We know that the global minimum is not found in the seven-structure-factor fit because, if we take the result given in Table 1, obtained using (1*b*), and minimize the χ^2 of (1*a*) using this as a starting point, we find a lower final value of χ^2 than in any of the random-start runs. As (1*c*) shows, once the match between I_{ex} and I_{th} is good, giving a low final value of χ^2, the results using (1*a*) and (1*b*) must be similar. At present we have no explanation for the different behaviour of the (1*a*) and (1*b*) functions. With the use of the improved minimization schemes discussed above, it is expected that the problem of local minima experienced with (1*a*) and (1*b*) will be considerably reduced.

Table 1. *Structure-factor amplitudes, a, and phases, φ, derived from the minimization of* χ^2

Parameter	Ideal results	Number of structure factors 4	5	6	7	8	10
$a_{1\bar{1}1}$	2.6322	3.0365	2.8277	2.8463	2.6766	2.6115	2.6178
a_{002}	0.5101	0.7766	0.6388	0.3719	0.4368	0.6639	0.5639
φ_{002}	1.8476	1.5317	6.1361	2.4890	1.2337	1.9182	1.9450
$a_{2\bar{2}0}$	−2.2645	−3.0897	−3.3738	−2.7793	−2.4881	−2.1763	−2.2164
$a_{1\bar{1}3}$	1.3659	1.6877	1.5327	1.5616	1.7286	1.5771	1.4563
$\varphi_{1\bar{1}3}$	3.8047	4.1204	3.7223	3.9153	3.9835	3.9293	3.8655
$a_{2\bar{2}2}$	0.4675	-	1.3154	0.4842	0.6510	0.5023	0.4426
$\varphi_{2\bar{2}2}$	1.8472	-	1.6334	1.5838	1.3570	2.1589	1.8814
a_{004}	1.4762	-	-	1.7465	1.4685	1.4503	1.5167
φ_{004}	0.5252	-	-	0.8493	0.9415	0.5779	0.4725
$a_{3\bar{3}1}$	0.9759	-	-	-	1.4826	1.1929	1.2117
$\varphi_{3\bar{3}1}$	6.1182	-	-	-	0.0009	0.0321	6.2067
$a_{2\bar{2}4}$	1.1213	-	-	-	-	1.8117	1.2992
$\varphi_{2\bar{2}4}$	0.5529	-	-	-	-	0.6308	0.7098
$a_{1\bar{1}5}$	0.7514	-	-	-	-	-	0.7393
$\varphi_{1\bar{1}5}$	3.5123	-	-	-	-	-	3.2525
$a_{3\bar{3}3}$	0.7696	-	-	-	-	-	0.6606
$\varphi_{3\bar{3}3}$	3.8859	-	-	-	-	-	3.9043
SSQ	-	0.3879	0.2750	0.1629	0.0855	0.0215	0.0042

The projected potentials constructed from the 'best fit' values of Table 1 are shown in Fig. 2. It should be emphasized that the results of Table 1 and Fig. 2 are obtained with essentially *no* prior knowledge of the crystal structure. Table 1 indicates that the largest errors tend to be found in the last added structure factor; in effect this least-significant structure factor 'soaks up' the errors in the lower-order U_G. It can be seen that an excellent representation of the

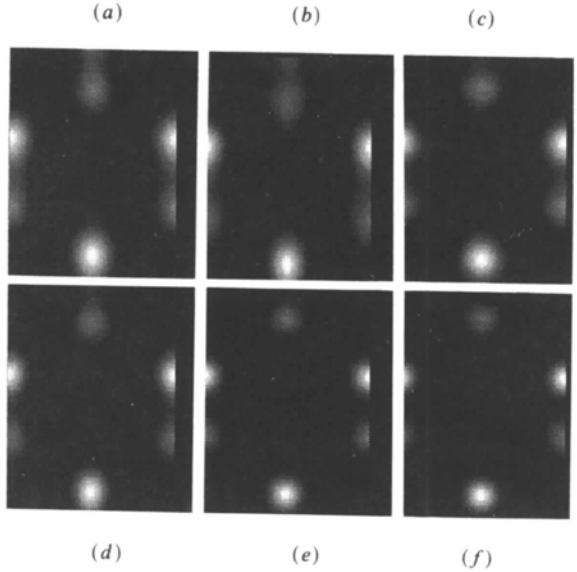

Fig. 2. Projected potentials derived from the best fits to the CBED pattern of Fig. 1(*b*). (*a*) Including $(1\bar{1}1)$, (002), $(2\bar{2}0)$ and $(1\bar{1}3)$ structure factors. (*b*) Adding $(2\bar{2}2)$. (*c*) Adding $(4\bar{4}0)$. (*d*) Adding $(3\bar{3}1)$. (*e*) Adding $(2\bar{2}4)$. (*f*) Adding $(1\bar{1}5)$ and $(3\bar{3}3)$.

projected potential is obtained with six structure factors (Fig. 2*c*) and that with ten structure factors the projected potential is almost perfect [compare Figs. 1(*d*) and 2(*f*)].

4. Discussion

Although we have been working with a much simplified example, our results indicate that the *ab initio* inversion of a CBED pattern appears to be feasible. However, a number of problems will arise when we attempt to apply the techniques described here to real experimental data. It is first necessary to consider the effects of HOLZ reflections and absorption. Neither of these present real difficulties. It is straightforward to include HOLZ reflections in the many-beam equations (*e.g.* Bird, 1989) and the calculation of gradients is not significantly changed. When including the effects of absorption we have to be careful with the non-Hermitian character of the many-beam matrix, but gradients can still be calculated, using both the left- and right-hand sets of eigenvectors (Bird & Saunders, 1992). More fitting parameters will also arise because each structure factor has an elastic and absorptive part, and these must be varied separately (Zuo & Spence, 1991). The inclusion of the thickness and the normalization constant as fitting parameters is again straightforward, because their gradients are simple to calculate. The main problem with making the theoretical model more realistic is that the size of the calculation increases dramatically, with respect to both the number of beams in the many-beam equations and the number of fitting parameters that are used in the minimization of χ^2. We are currently investigating two methods that might allow the computing time required by the minimization to be reduced. Firstly, better minimization strategies such as simulated annealing or 'kicking out' from local minima should make it easier to find the global minimum using considerably fewer than the 150 runs used here. Secondly,* when initializing the minimization run, we could use atomicity criteria (as used in X-ray direct methods) to generate physically reasonable combinations of starting structure factors rather than the totally random start points presently used. With current advances in computer power, we believe that full-size calculations will be possible in the near future.

Although our analysis has concentrated on the *ab initio* inversion problem, the methods described here can be applied equally well to the refinement of low-order structure factors in a known crystal. In fact, the minimization of χ^2 is easier in this case because the starting point is well defined and the problem of local minima is reduced, if not eliminated completely. The advantages of zone-axis diffraction over systematic diffraction discussed in § 1 also apply equally well to structure-factor refinement and it is expected that many-parameter zone-axis refinement, performed using quasi-Newton minimization, will significantly extend existing refinement techniques (Zuo & Spence, 1991).

Finally, the analysis in this paper has used simulated patterns instead of real experimental data. Any real data will have noise, as well as an unavoidable thermal diffuse background that is not removed by energy filtering. Tests are currently under way to assess the influence of noise and background and the first indications are that the addition of random noise to our 'experimental' intensities has little effect on the final results. This is to be expected, given that (as discussed above) the problem is highly over-determined. The more crucial test, of using real experimental data, will be done as soon as digitally collected energy-filtered zone-axis patterns become available.

This work is supported by the Science and Engineering Research Council.

* We are grateful to one of the referees for suggesting this.

References

BIRD, D. M. (1989). *J. Electron Microsc. Tech.* **13**, 77-97.

BIRD, D. M. (1990). *Acta Cryst.* A**46**, 208-214.

BIRD, D. M., JAMES, R. & PRESTON, A. R. (1987). *Phys. Rev. Lett.* **59**, 1216-1219.

BIRD, D. M. & KING, Q. A. (1990). *Acta Cryst.* A**46**, 202-208.

BIRD, D. M. & SAUNDERS, M. (1991). In *Microbeam Analysis* 1991, edited by D. G. HOWITT, pp. 153-156. San Francisco Press.

BIRD, D. M. & SAUNDERS, M. (1992). In preparation.

DOYLE, P. A. & TURNER, P. S. (1968). *Acta Cryst.* A**24**, 390-397.

FLETCHER, R. (1987). *Practical Methods of Optimization.* London: Academic Press.

GILL, P. E., MURRAY, W. & WRIGHT, M. H. (1981). *Practical Optimization.* New York: Wiley.

GJONNES, J., BOE, N. & GJONNES, K. (1990). In *Electron Microscopy* 1990. *Proc. XIIth ICEM*, edited by L. D. PEACHY & D. B. WILLIAMS, Vol. 2, pp. 516-517. San Francisco Press.

MARTHINSEN, K., HOIER, R. & BAKKEN, L. N. (1990). In *Electron Microscopy* 1990. *Proc. XIIth ICEM*, edited by L. D. PEACHEY & D. B. WILLIAMS, Vol. 2, pp. 492-493. San Francisco Press.

MAYER, J., SPENCE, J. C. H., ERNST, F. & MÖBUS, G. (1991). In *Proc. 49th Annu. Meet. EMSA*, edited by G. W. BAILEY, pp. 786-787. San Francisco Press.

TAFTØ, T. & METZGER, T. H. (1985). *J. Appl. Cryst.* **18**, 110-116.

TANAKA, M. & TSUDA, K. (1990). In *Electron Microscopy* 1990. *Proc. XIIth ICEM*, edited by L. D. PEACHY & D. B. WILLIAMS, Vol. 2, pp. 518-519. San Francisco Press.

TANAKA, M. & TSUDA, K. (1991). In *Microbeam Analysis* 1991, edited by D. G. HOWITT, pp. 145-149. San Francisco Press.

TOMOKIYO, Y. & KUROIWA, T. (1990). In *Electron Microscopy* 1990. *Proc. XIIth ICEM*, edited by L. D. PEACHY & D. B. WILLIAMS, Vol. 2, pp. 526-527. San Francisco Press.

VINCENT, R. & BIRD, D. M. (1986). *Philos. Mag.* A**53**, L35-L40.

VINCENT, R., BIRD, D. M. & STEEDS, J. W. (1984). *Philos. Mag.* A**50**, 765-786.

VINCENT, R. & EXELBY, D. R. (1990). In *Electron Microscopy* 1990. *Proc. XIIth ICEM*, edited by L. D. PEACHY & D. B. WILLIAMS, Vol. 2, pp. 524-525. San Francisco Press.

ZUO, J. M. (1991). *Acta Cryst.* A**47**, 87-97.

ZUO, J. M. & SPENCE, J. C. H. (1991). *Ultramicroscopy*, **35**, 185-196.
ZUO, J. M., SPENCE, J. C. H. & HOIER, R. (1989). *Phys. Rev. Lett.* **62**, 547-550.
ZUO, J. M., SPENCE, J. C. H. & O'KEEFFE, M. (1988). *Phys. Rev. Lett.* **61**, 353-356.
ZUO, J. M., SPENCE, J. C. H. & PETUSKEY, W. (1990). *Phys. Rev. B*, **42**, 8451-8458.

Acta Cryst. (1992). A**48**, 562-568

Dynamical Scattering and Electron Crystallography – *Ab Initio* Structure Analysis of Copper Perbromophthalocyanine

BY DOUGLAS L. DORSET

Electron Diffraction Department, Medical Foundation of Buffalo, Inc., 73 High Street, Buffalo, New York 14203, *USA*

AND WILLIAM F. TIVOL AND JAMES N. TURNER

Wadsworth Center for Laboratories and Research, New York State Department of Health and School of Public Health, University of New York at Albany, Albany, New York 12201-0509, *USA*

(*Received* 30 *September* 1991; *accepted* 11 *February* 1992)

Abstract

Electron diffraction intensity data were collected at 1200 kV from thin epitaxially oriented crystals of copper perbromophthalocyanine ($C_{32}Br_{16}CuN_8$) in a projection down molecular columns. Measured cell constants for the projection with *cmm* symmetry are $d_{100} = 17.88\ (9)$, $b = 26.46\ (15)$ Å. The structure was determined by Fourier refinement after three heavy-atom positions were identified in an initial potential map. In addition to the copper and halogens, all light-atom positions were found. Although the final R value for all data is 0.41, n-beam dynamical calculations for crystal thicknesses corresponding to the estimated sample dimension account for the observed amplitudes that deviate most from their kinematical values.

Introduction

Is electron crystallography possible? That is to say, can electron diffraction intensity data from thin microcrystals be exploited for quantitative *ab initio* structure analyses in much the same way as X-ray crystal-structure determinations are carried out? Since the early work of Rigamonti (1936), there have been numerous attempts to answer this question, including the comprehensive program on organic compounds begun by Vainshtein and his co-workers in Moscow (Vainshtein, 1964).

Although the first use of direct phasing techniques to solve a structure with electron diffraction intensities was reported 15 years ago (Dorset & Hauptman, 1976), only recently has successful application of this technique to a number of representative organic structures shown (Dorset, 1991) that the above questions can be answered affirmatively if the compounds investigated are composed of light atoms such as carbon, nitrogen and oxygen. These analyses show that, after initial determination of atomic positions, the structures can be refined by Fourier techniques (and possibly also constrained least-squares techniques) to produce a reasonable packing scheme in which the constituent molecules are found to have chemically meaningful bond distances and angles. If microcrystals are the only preparations available (as in linear polymers), electron crystallographic techniques can be used to obtain reasonably accurate molecular architectures.

Because of dynamical scattering, the presence of heavy atoms in an organic structure may, on the other hand, make a structure analysis difficult or impossible. This was anticipated by the direct phasing analysis of simulated electron diffraction data from the disodium salt of an organic sulfinate (Dorset, Jap, Ho & Glaeser, 1979). Analysis of a 60 kV data set from thiourea (Dvoryankin & Vainshtein, 1960) has shown that the phase estimates obtained from the computed triplet and quartet structure invariants are correct, but the dynamical-scattering contribution from the sulfur atom can affect the accuracy of bond distances and angles calculated from the atomic positions found in the potential maps (Dorset, 1991). Use of shorter electron wavelengths may be helpful, as demonstrated in the structure determination of copper perchlorophthalocyanine with high-voltage electron diffraction intensity data. By low-dose electron

0108-7673/92/040562-07$06.00